DOI: 10.24996/ijs.2019.S.I.18

ISSN: 0067-2904

Effects of TEOs aerogel particles size of TEOS aerogel on its mesoporous structure and thermal behavior via supercritical drying and high temperature

Ashraf M. Ibrahim[1*], Baha T. Chiad[2], Wesam A. A. Twej[2], Ruaa A. Mohammed[1]

[1]Department of Medical Instruments Techniques and Engineering, AL Hussain University College, Karbala'a, Iraq

[2]Department of Physics, College of Science, University of Baghdad, Baghdad, Iraq

Abstract

TEOS aerogel a is the most commonly used. a Aerogel has attracted increasing attention from both academic and industries due to its extraordinary performance and potentials. We have systematically studied the relationship between the densification temperature of the synthesis environment of silica aerogels on their resulting morphological, optical and thermal properties. SEM and BET measurements were employed as structural probes to ascertain the structural differences. Lee's disc apparatus was used for determining the thermal conductivity coefficient. There is a systematic correlation between the annealing temperature and the aerogel surface area, porosity, as well as pore size. The implemented autoclave was able to produce aerogel monolith of surface area reaching to 998.25 g/m2 and low electric conductivity arrive to of 1.17*10-4(s/m), associated with density of 0.047 g/cm3.The calculated thermal conductivities were (0.0063, 0.016 and 0.0053 mW m-1 0 C-1) for pH1, pH7 and pH8 samples respectively. The microstructure observed is categorized into three types, namely, open cellular foam (the substance that is formed by trapping pockets of gas in solid), fractal (the structural features it's clearly show the hierarchical repetition) and isotropic morphology (visible spectrum scale). The aerogel properties were are remarkably varied. While the influence of annealing temperature the reaction setting has gradually influence on the final aerogel properties, h However, it is obviously requested for achieving desirable optically and nano-featured products.

Keywords: Aerogel, BET, Autoclave, transmittance.

تاثير حجم الجسيمات على الهيكلية المسامية للهلام الهوائي والسلوك الحراري عن طريق التجفيف فوق الحرج ودرجة الحرارة العالية

أشرف محمد العطار[1*]، بهاء طعمة جياد[2]، وسام عبد علي تويج[2]، رؤى علي محمد[1,2]

[1]قسم هندسة تقنيات الاجهزة الطبية، كلية الحسين الجامعة ، كربلاء، العراق

[2]قسم علوم الفيزياء،كلية العلوم، جامعة بغداد، بغداد، العراق

الخلاصة

قد اجتذب سليكا الهلام الهوائي (الايروجل) اهتماما متزايدا باعتبارة الاكثر شعبية بين الاوساط الاكاديمية والصناعية . كل ذلك يرجع الى الاداء والامكانيات الغير اعتيادية الاستثنائية التي يمتلكها هذا النوع من السليكا. حيث درسنا بشكل منهجي العلاقة بين درجة حرارة التكثيف في بيئة التوليف النتاجة على خصائص سيليكا الايروجل التركيبية والبصرية والحرارية . تم استخدام كل من المسح الالكتروني المجهري وذلك

*Email: dr.ashrafibrahim@huciraq.edu.iq

الامتصاص الامتزاز بواسطة النتروجين السائل كتحقيقات هيكلية للتاكد من الاختلافات التركيبية. كما تم اتسخدام جهاز القرص(لي) لاجل تحديد معامل الموصلية الحرارية. تبين ان هنالك علاقة منهجية بين كل من درجة حرارة التلدين ومساحة السطح.حيث تمكن الاتولكيف (حجر الضغط) المصنعمن انتاج كتلة متراصة من الهلام الهوائي بمساحة سطحية تصل 998,25 غم/ م2 وتوصيلية كهربائية منخفضة تصل الى 1.17*10−4 غم/سم3. كانت التوصيلية الحرارية لعينات الرقم الهيدروجي (1,7,8) المحسوبة على التوالي هي (0.0063 و 0,061 و0,0053 ملي واط م−1 س−1.(

تم تصنيف العينات حسب حسب البنية المجهرية الموضحة الى ثلاث انواع, وهي:

ذو الرغوة الخلوية المفتوحة(مادة صلبة تتشكل من خلال احتجاز الجيوب الغازية) , والكسورية الهرمية (وهي من السمات الهيكلية التي تضهر بوضوح من خلال التكرار الهرمي) و التشكيل المتماثل (مقياس الطيف المرئي). حيث اضهرت نتائج الفحص تنوع ملحوظ في خصائص الهلام الهوائي (الايروجل). على الرغممن تاثير درجةحرارة التلدين قد اثرت تدريجيا على الخصائص النهائية للهلام الهوائي . الا انه من الوضح انه مطلوب وذلك لاجل تحقيق منتج نانوي مرغوب من الناحية البصرية والنانوية.

1. Introduction

The rough last decades noticed development in the technique of the sol-gel that has led to fast rapid progress in the deliberate synthesis of porous materials. Silica alcogel can be processed by using different ways to yield aerogels; the approach taken in this work is to produce the silica aerogel was by the supercritical drying method (SCD) [1, 2].

These types of materials are of immense importance t in different applications like absorption, sensing, catalyst, etc. Silica aerogel become quite popular among all other materials, It was first silica aerogel was produced first in the 1930. In the first half of the century (1931, Kistler)[3]. During the last decade the synthesis of aerogel has received a significant attention because of its possession ing of a number of unusual physical properties that has attracted the attention of researchers. Aerogel properties are known to be highly dependent on the initial conditions [4]. Many fascinating properties found in aerogel, is a nanostructured material and . a According to itstheir structure aerogel have with specific of has high surface area, very low density, and extremely high porosity. Silica aerogels are materials with unusual properties such as high specific surface area (500–1200m2/g), high porosity (80–99.8%), low density (~0.003 g/cm3), high thermal insulation value (0.005W/mK), ultra-low dielectric constant (k = 1.0 – 2.0) and low index of refraction (~1.05) [5-8]. Based on these properties many different fields of application of silica aerogel have been reported [9, 10]. Thermal treatment is one of these parameter s that has ve an influence on the structure of aerogel. In this study, silica aerogel was prepared by used the supercritical drying(SCD) by using CO2 . t This process give has an advantage of not causingto avoid the capillary stress and the associated drying shrinkage. The densification process of silica aerogel at high temperature is the last stage of aerogel processes. In order to interpret the effect of temperature, it is important to study the effect densification of silica aerogel at various temperatures. Using tetraethylorthosilicate (TEOS) for 1 pH value to measure the pores size, pore volume and surface area were measured,. also see t The transparency of each sample at different temperature was alsostudied. In this work, there are four different regions which were identified from the characterizations of the samples. These R regions are exhibited a structure densification of bulk at room temperature, 500 0C, 7000C and at 900 0C. These regions of temperatures show the optical transparency and structures of aerogels samples will be change during change of temperatures of densification.

Experimental

2.1. Materials

Synthesis of aerogel is used was done using different chemical materials which were, tetraethylorthosilicate ((TEOS) with > 99.0% purity), spectroscopic grade ethyl alcohol (200 proof > 99.5% purities, N, N, dimethaylformamide ((C3H7NO)> 99.0% purity) deionized water catalyzed by ammonium fluoride (> 98.0% purity).

2.2. Procedure

The gels of silica were produced t via through a single-step procedure as followsing; : TEOS, ethanol, water, and hydrochloric acid (volume ratios 2.5:10:2: N) where N was varied to achieve final

sol of pH1were mixed together. Under magnetic stirring, the sols were heated at 303 K for 30 min. Then 0.5 ml of C3H7NO, was added ing as a drying control chemical additive (DCCA) and left stirring for further 1 hour.

The resulted ing give rise to gel is in of 3.2 cm diameter tubes of plastic and aged at temperature of room for 36 h. In order to get pure ethanol in five 24h, gel be washed to get remove al for any unreacted monomer from networks.

supercritical drying of the gel was conducted in specially designed reactor capable of withstanding high pressures at pressure of 1100- 1215 psi and a temperature of 450C for 4 hours. During this process it is necessary to provide optimum mixing between supercritical CO2 and the solvent that exists in the pores of the gel. With the end of SCCO2, drying , the densification s at its last stage and that was made performed with four different temperatures, room temperature, 500 0C, 7000C and 9000C. Camera p Photos of or the implemented autoclave system as well as the aerogel samples that were prepared under different pH values are presented in Figure-1.

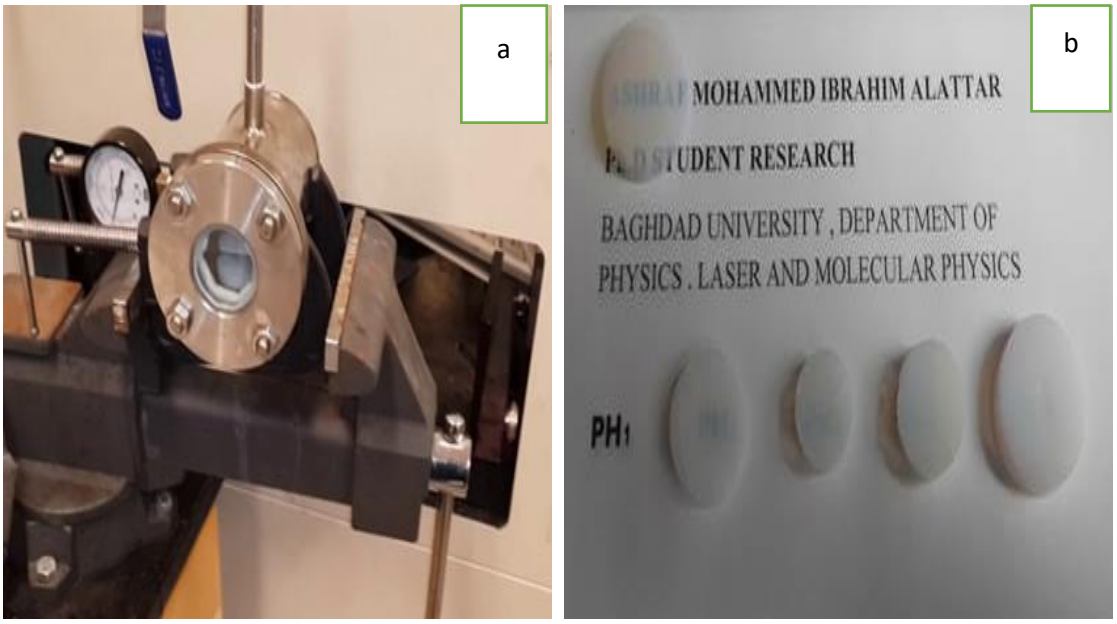

Figure 1-Camera image forPhotos of (a) Implemented autoclave, (b) some aerogel samples with their preparation pH1 value.

2.3. Characterization of aerogels.

The pore size allocation, pore volume and specific surface area of aerogel specimens were determined by Brunauer–Emmitt–Teller (BET) method (micromeritics ASAP 2020).

The morphology and microstructures of silica aerogels specimens were observed by with a scanning electron microscope y (SEM, ULTRA 60) in secondary electron mode.

UV-VIS spectrophotometer (Ultrospec. 4300 pro) was used in this work to record the transmittance of the aerogel samples. FT-IR spectrophotometer (Nicolet Is50) was used to collect s high spectral resolution data for samples of aerogel over the spectral range from 400 cm-1 to 4000 cm-1. A.C conductivity device was used for to investigate ing the behavior of conductivity and the dielectric material of disc aerogel. Measurements were done with, A Hewlett. Packard-R2C unit model (4275 A), multi frequency LCR meter has been used to measure the capacitance (C) and resistance (R) with frequency range between 100Hz-100kHz.

By weighing cylindrical uniform aerogel samples of precise dimensions, the apparent densities were calculated. The dried aerogels were then annealed by heating with to different temperatures at a rate of 60 °C /h-1.

3.Results

3.1. Surface area and pore size measurements

Various catalyst systems were characterized by BET nitrogen adsorption-desorption, used to obtain pore volumes and surface areas of the silica aerogel. Utilizing BET analysis method was used to found find the pore volume using a single condensation point (P/Po = 0.99) and while five points (0.05

<P/Po < 0.35) were undertaken to obtain surface areas. The desorption isotherm method was used to calculate pore size distribution. Nitrogen adsorption surface areas were iterative on the same specimens and were found to not deviate no deviation from the previous measurementswas found except from more than the expected error of the tests (± 5%), indicating that the small-scale structure does not collapse as a result of canicular pressure from the nitrogen.

The linear isotherm plots for the aerogel samples prepared at several densification temperatures (non-densification, 500 0C, 700 0C, 900 0C) at final pH= 1Ph 1 value are presented in Figure-2, which shows T the effect of temperature on the each of surface area, pore size, and pore volume are displayed in Figure-2. In general, the surface area of silica aerogels increases as temperature of densification increases, as shown that in Table-1 that demonstrates the variation of pore volume and size with final temperature of densification of preparation at PhpH=1 value.

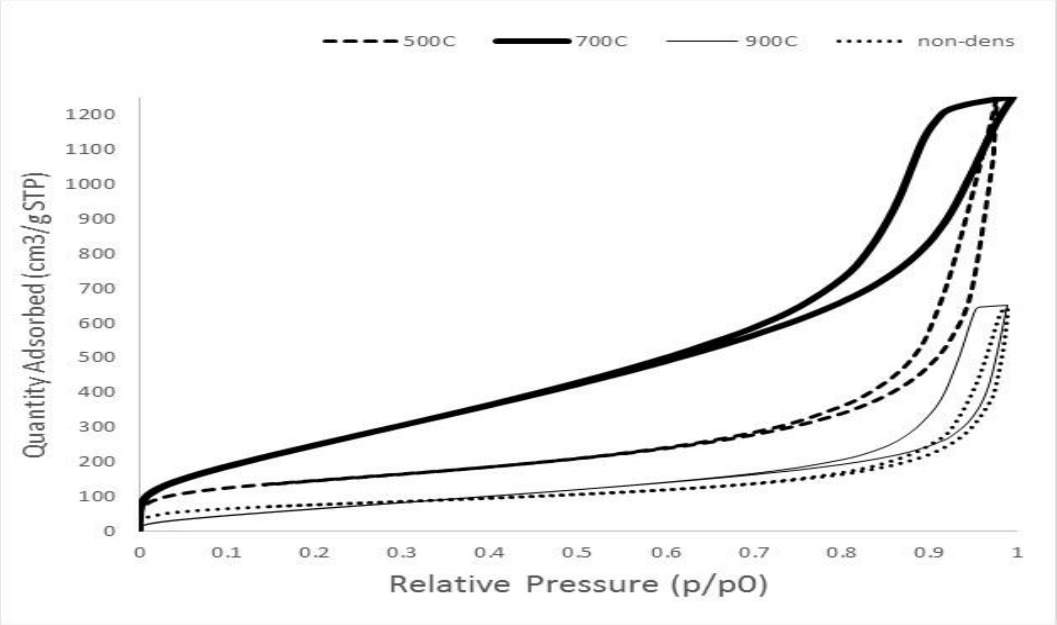

Figure 2-Linear isotherm plots for aerogel prepared at initial Ph=1 with different temperatures of densification.

Table-1summarized t The nitrogen sorption measurements for the silica aerogel prepared under pH =1 value with non-densification and at 5000C, 700 0C and 900 0C of densification temperatures.

Temp (^{0}C)	**Surface area (m^2/g)**				**Pore volume (cm^3/g)**			**Pore size (Å)**		
	BET	**Single**	**BJH ADS**	**BJH DES**	**Single**	**BJH ADS**	**BJH DES**	**Single**	**BJH ADS**	**BJH DES**
Non-dens	**279.27**	**268.24**	**250.69**	**257.27**	**0.58**	**0.99**	**1.00**	**83.13**	**158.56**	**156.62**
500	**531.28**	**511.95**	**523.17**	**557.14**	**1.62**	**2.55**	**2.54**	**12.19**	**19.54**	**18.29**
700	**998.25**	**934 .18**	**1011.09**	**1105.61**	**1. 93**	**1.79**	**1.82**	**7.771**	**7.101**	**6.593**
900	**282.75**	**254 .59**	**322.83**	**356.27**	**1. 01**	**0.97**	**0.98**	**14.272**	**12.126**	**11.055**

The influence of the densification temperatures of at pH=1 value on the surface area, pore size & and volume are is clear through the Table-1). The Table-1 show It elucidates d the distinction of pore volume and pore size for final densification temperatures at pH=1 value. Without densification yielding maximum pore size, lowest pore volume and surface area were obtained, while the densification of aerogel under 700 0C yields ing product of the minimum pore size,but highest pore

volume and surface area pore volume and surface area highest,. i On the other hand the 500 0C results are in between the previous results is the moderate between of both.

In other hand, t The influence of densification on the densities of aerogel bulks is summarized in the Table-2.

Temp ^{0}C	**Mass (gm)**	**Radius (cm)**	**High (cm)**	**Density ρ (g/ cm3)**
Non-dens	0.2381	2.7	0.75	**0.055**
500	0.2243	2.7	0.75	**0.052**
700	0.2169	2.7	0.75	**0.050**
900	0.2021	2.7	0.75	**0.047**

Table -shows the m Mass, radius, thickness and density values for aerogel bulk samples before and after densification at three different temperatures.

Through the step of densification, it is observed that there are varied differences in the density of these samples regarding to their temperatures of densification.

3.2. Morphology.

Figure-3 shows the SEM images of aerogel samples with pH=1 value with non-densification and with densification temperatures of at 500 0C, 700 0C and 900 0C. The at images show that the samples of aerogel have different network structures related to the densification temperatures. The morphology of these samples is classified into three distinct categories. It The morphology of the four samples can be grouped into three distinct categories, fractal (M1), isotropic (M2), and open cellular foam (M3).

The non-densification and 500 0C specimens has two too similar microstructures that are easily manifested to be fractal in ease. The microstructure at of the 700 0C sample shows ultrafine nanoscale structure at the nanoscale, but it is fairly isotropic at the 10 and 300 nm scale. At 900 0C, the microstructure of aerogel sample shows the open cellular foam structure.

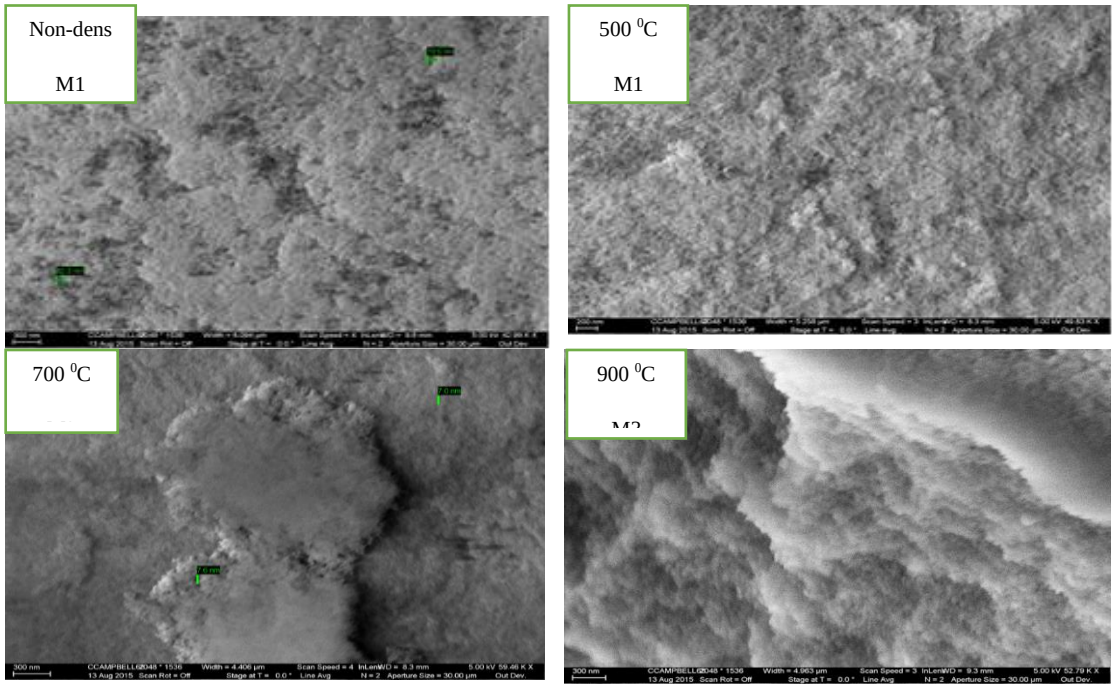

Figure 3-SEM images for of aerogel specimens prepared of pH=1, at different densification temperatures.

3.3. UV-VIS spectroscopy

Figure-4 resents the transmittance of aerogel samples as a function of wavelength at final preparation of pH=1 value at different densification temperatures. Interestingly, non-densification and at 900 0C aerogel samples exhibit minimum transmittance in the entire VIS region, whereas at 700 ^{0}C sample show higher transmittance at higher wavelength, and but at 500 ^{0}C the sample of aerogel has have intermediate values.

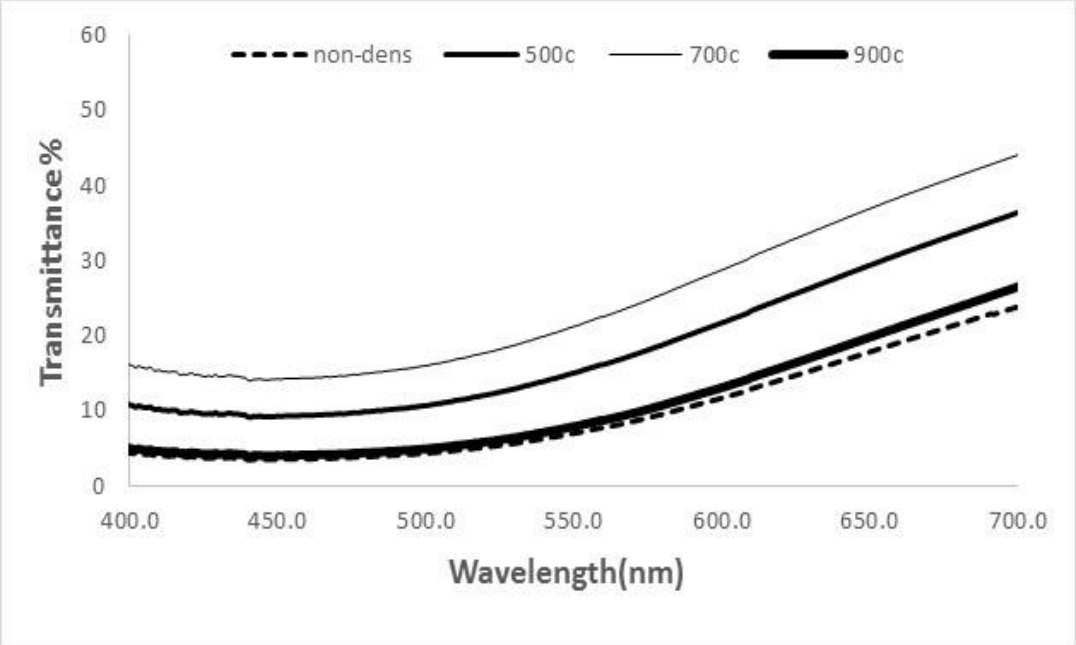

Figure 4-Transmittance spectra for aerogel samples at different densification temperatures.

3.4 FT-IR spectroscopy

The recorded IR transmitted spectra for the prepared aerogel specimens are shown in Figure-5. Several absorption bands are marking pointed out in these spectra due to their interesting importance in our study.

FTIR transmission spectra for aerogel sample pH=1 at three different annealing temperatures; 500 °C, 700 °C and 900 °C is are shown in Figure-5.

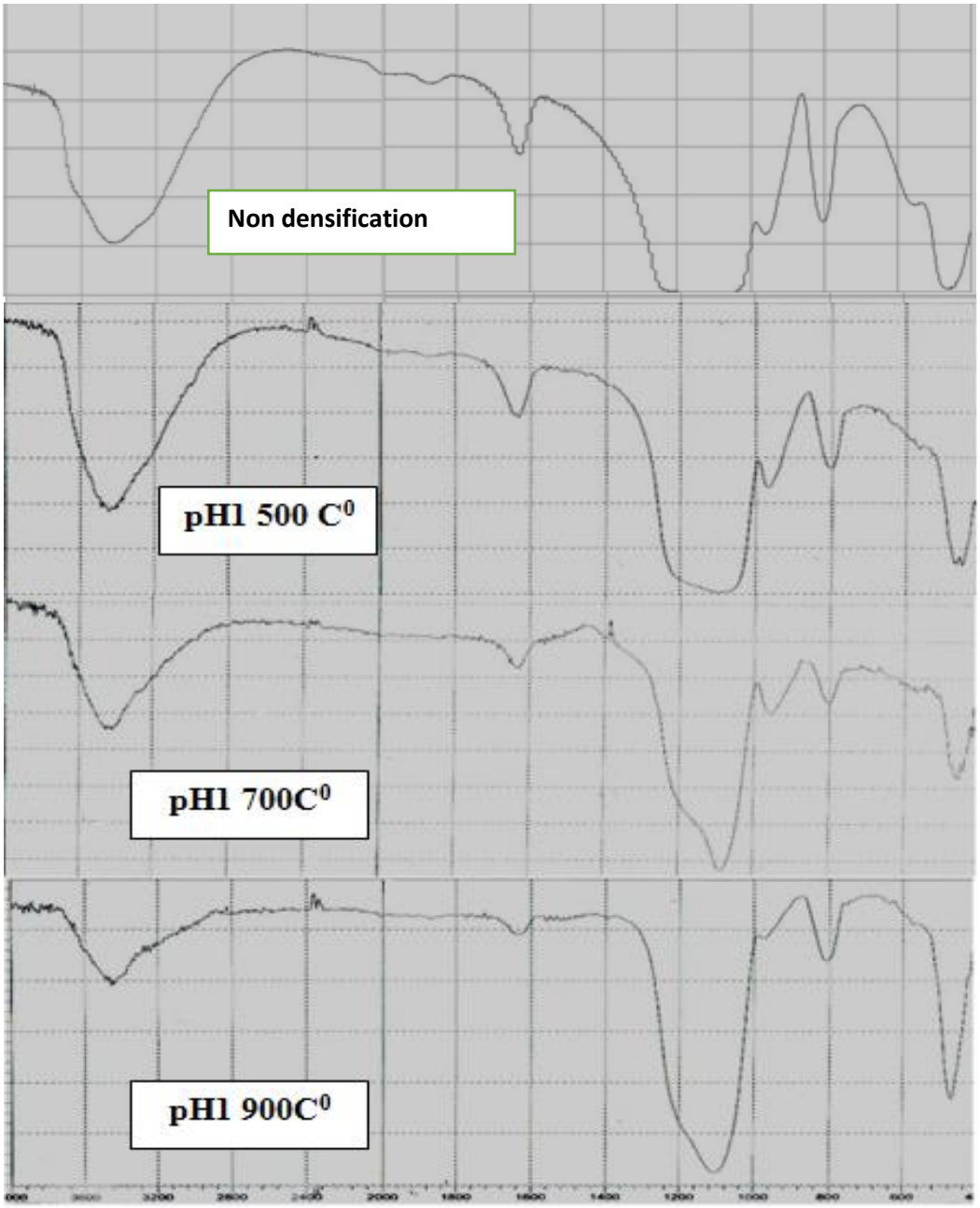

Figure 5-FTIR transmission spectra for aerogel sample pH=1 at three different annealing temperatures 500 °C, 700 °C and 900 °C.

3.5 Thermal conductivity

Thermic conductivity tests for the aerogel samples were carried out via the by Lee's Disc technique of aerogel samples. The heat transfers between an aerogel bulk and its surroundings depend on the exposed surface area of aerogel specimens and temperature divergence between the bulk aerogel and its surroundings.

To characterize thermal conductivity of the aerogel samples ,chose three samples were chosen at different pH values, acidic pH=1, natural pH=7 and basic environment pH=8 samples. Figure-6) present cluster columns of thermal conductivity for aerogel selected samples. The calculated thermal conductivities were (0.0063, 0.016 and 0.0053 mW m-1 0 C-1) for pH=1, pH=7 and pH=8 samples, respectively (as shown in Figure-6).

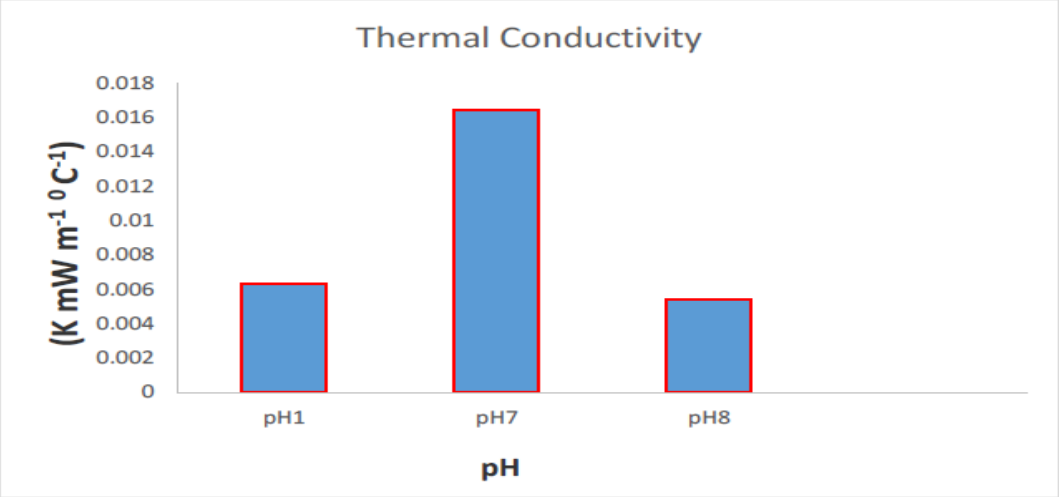

Figure 6-columns images thermal conductivity of aerogel specimens prepared with pH=1, pH= 7 and Ph= 8 solutions

Figure-7 demonstrates the behavior matching between silica aerogel thermal conductivity, density and reveres matching with porosity.

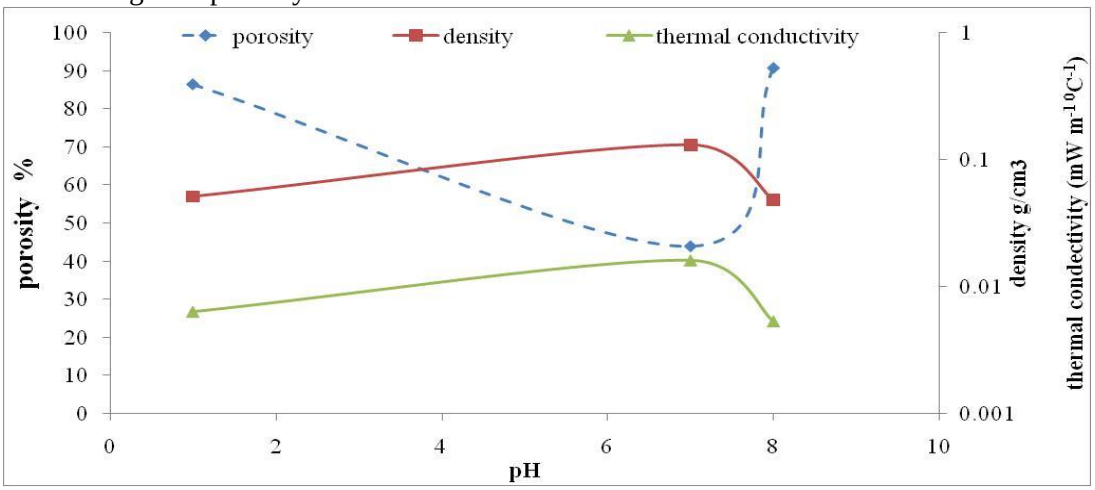

Figure 7-porosity,density and thermal conductivity variation according to preparation at pH =values 4.

4. Discussion

In t This work we focused, in our examination, on four samples which can were represented without densification and with densification at 500 ^{0}C, 700 ^{0}C and 900 ^{0}C, respectively.

The linear isotherm plots (which are presented in Figure-2 can be examined with the aid of the IUPAC classification hysteresis loops [11]. The plots of samples of pH=1, at 700 ^{0}C and 900 ^{0}C that shown in Figure-2 it are classified ying as H3 type (slit-shaped pores) which is concerning indicates to non-rigid aggregates of plate-like particles. The plots belonging to pH=1, without densification and at densification temperature 500 ^{0}C Figure-2 that can be categorized as H1 type, which shows that pore channels have well-defined cylindrical shape. Except at 500 ^{0}C densification temperature of aerogel sample, low densification temperature and high densification temperature behaviour showing through two branches of the linear isotherm plot. approximately at 700 ^{0}C, at 900 ^{0}C, to be exact silica has its isoelectric point (IEP). At the IEP, the reaction rate for condensation is at a minimum; hence the water condensation mechanism becomes favourable [12].

This status might be giving give rise to less branchy networks and command to large pore sizes, resulting in a sufficient adsorption quantity at high relative pressure.

Belong to At pH=1 and the densification temperature control, therefore, strongly affect the resulting microstructure, and will allow for the surveillance of microstructure-dictated properties. Aerogel transmittance spectra, in the entire VIS region of pH=1at different temperature of densification, samples are shown in Figure-4. It is clear that sample the non- densification sample exhibit minimum transmittance whereas pH=1 aerogel samples at 500 ^{0}C and at 900 ^{0}C show a

moderated value and while the sample at 700 ^{0}C demonstrates the highest r transmittance. Highly transparent aerogels are normally prepared using a two-step method [13,14]. With this work, a single step process was utilized in preparing ed the specimens utilizing process of a single step in order to minimize the number of synthesis factors and therefore better establish the effect of annealing on the resulting aerogels is better established.

Subsequently, all specimens are made solely of silica, therefore, the structure of silica aero-gel network is the individual factor and that will be giving rise for any difference in the transmittance (Fig. (4)). The variation of refractive index of silica network and pore material may be a reasonable source of light scattering, where pores work as the scattering centers. The specimens transmittance values of the specimens at each densification temperature are were normalized through the total transmittance for of that sample. Since the light absorption coefficient of light by silica in the visible region is small, the attenuation of light should result from is due to scattering from the aerogel structure [15]. When the in homogeneities inhomogeneities of the aerogel network are smaller than the visible light wavelengths, nearly isotropic light (Rayleigh) scattering is expected. The resulting microstructure would be M2, from the three canonical structures (M1-M3) identified in Figure-3.The presence of microstructural elements that are on the order of the optical wavelengths, such as those found in the M1 microstructure, because of Mie scattering. The short-range fractal structures and the strongly localized vibrations of that structure also contribute significantly to scattering; the fractal structures scatter significantly as shown in the work by of Alexander [16]. The maximum of this scattering was shown to occur when the wavelength is close to the size of the fraction. The M1 microstructure from shown in F fig. (3) is of this type typifies this fractal microstructure and.It is observed in the aerogel samples non-densification and at 500 ^{0}C and non-densification. The recorded IR transmitted spectra for the prepared aerogel samples are shown in Fig. (3). Several absorption bands are marked ing out in these spectra due to their interesting importance in our study. There are T two vibrational bands of aerogel silica that appeare appears d in the region of the FTIR spectrum of fingerprint, strong centered at around 460 cm-1, and strong and broad at 1104 cm-1that are. These corresponds ing to the bending and to the asymmetric stretching vibrations of (Si—O—Si) groups, respectively, w While the symmetric stretching characteristic silica band is weak and has appeared at 812 cm-1¬ [17].

Medium and broad O–H vibrations at 3,500 cm-1and small sharp at 1,650 cm1 indicate the presence of residual free OH groups (or adsorbed) within the aerogel [18].

FTIR spectra for aerogel sample pH=1 at four different annealing temperatures; 500 °C, 700 °C and 900 °C are presented in fig. (5). The weak band peak fixed at 965 cm−1 may be ascribed to stretching vibration of silanol (Si—OH) groups [19].

Monotonically the intensity of this peak start to decrease ing when the annealing temperature starts ed to increase of annealing temperature. This may be due to the completing of the condensation reaction with temperature yielding more and more conversion of silanol bonds to siloxan bonds (Si—O—Si) [19].

Figure-6 shows the thermal conductivity for silica aerogel at different pH. It is obviously clear that the average thermal conductivity of aerogel samples is well below that for of still air (0.024 mWm-1 ^{0}C-1). The increase ing in of solid components will decreases the thermal conductivity; therefore, low porosity as well as low density materials are always qualified as low thermal conductivity materials. Supercritical dried aerogels are usually characterized by their high porosity, low density. Therefore, Figure-7 that shows that thermal conductivity of silica aerogels can be governed through controlling their densities or porosities.

This may be due to the thermal insulation tendency of this material; therefore, it would not allow any transferring of thermal energy as a result of temperature gradient,. as As a consequence, heat is transferred by phonons (lattice vibration waves) which are unable to vibrate due to thermal energy.

Where When silica aerogel has three dimensional networks that make solids consist of very small particles linked in the aerogel network in three dimensional with many "dead ends". Therefore, the thermal transp transport arent through the solid portion of silica aerogel occurs through tortuous path and it is not particularly effective, leading to the low thermal conductivity in such type of materials.

In addition, the porous are not closed of the sample but open that will cause to the allow gas to pass age through and that is another reason for the low lowering the conductivity.

5. Conclusions

This work We demonstrated the a systematic correlation between the effect of annealing temperature and the resulting microstructure and optical properties of silica aerogels. Homemade simple designed autoclave can offer a Aerogel samples of proper physical properties were prepared using a homemade simple designed autoclave. The temperature densification influence on the aerogel produced yielding highly transparence lower density crackly monolith. At 700 ^{0}C yielded ing the best surface area, pore size, smaller particle size and pore volume, . w While maximum temperature of annealing gave ive the lowest density through the evaporation ed of all the liquid inside the pores which with changed in the optical and structural properties of aerogel. Therefore, several applications; low densities thermal insulator, optical window, small-pore hydrogen storage tanks etc., could be functionally through adjusting starting catalyst in addition to the effect temperature as the function of last step to produce the aerogel

Acknowledgements

We would like to acknowledge the National Science Foundation Nanostructured Materials for Energy Storage and Conversion (NESAC) IGERT program for traineeship support under Award Number 1069138. In addition, we thank the Iraqi Ministry of Higher Education and Scientific Research for their generous support.

References

1. Tamon, H., Kitamura, T., Okazaki, M**. 1998.** *Colliod Interf. J. Sci*. **19**: 353-359.
2. Rami, A.O., E. R. Houssam, E.R. **2010.** *App. Surf.Sci*. **257**: 276-281.
3. Kistler, S.S. **1931**. *Nature*, **227**: 741.
4. Ashraf, M. Alattar, Matthew Drexler, Wesam A.A. Twej, Faisal M. Alamgir. **2018**. Structural and luminescent properties of a NaYF4-aerogel composite. *Photonics and Nanostructures – Fundamentals and Applications*, **30**(2018): 65–72.
5. Kharzheev YN. **2008.** *Phys Part Nuclei*, **39**: 107–135.
6. Yoldas BE, Annen MJ. **2000**. *Bostaph, Chem. Mater*. **12**(8): 2475–2484.
7. Carraher Jr., C.E. **2005**. *Polym. News*, **30**(12): 386.
8. Schultz, J.M., Jensen, K.I. and Kristiansen, F.H. **2005.** *Sol. Energy Mat. Sol. Cells*. **89**: 275.
9. Jensen, K.I., Schultz, JM. and Kristiansen, FH. **2004**. *JNCS*, **350**: 351–357.
10. Bernik DL. **2007**. Silicon based materials for drug delivery devices and implants. *Recent Pat. Nanotechnol*., **1**(3):186–192.
11. Sing, K.S.W., Everett, D.H., Haul, R.A.W., Moscou, L., Pierotti, R.A., Rouquerol, J. and Siemieniewska, T. **1985.** Reporting Physisorption Data for Gas/Solid Systems with Special Reference to the Determination of Surface Area and Porosity," *Pure and Applied Chemistry*, **57**(4): 603–619.
12. Brinker, C.J., Sehgal, R., Hietala, S.L., Deshpande, R., Smith, D.M., Lop, D. and Ashley, C.S. **1994.** *Journal of membrane science*, **94**(1): 85-102.
13. Emmerling, A., Petricevic, R., Beck, A., Wang, P., Scheller, H. and Fricke, J. **1995.** *Journal of Non-Crystalline Solids*, **185**(3): 240-248.
14. T. M. Tillotson, T.M. and Hrubesh, W. **1992.** *Journal of non-crystalline solids*, **145**(1-3): 44-50.
15. Athmuri, K. and Marinov, V. **2012.** *Advances in materials science*, **12**(1): 5-16.
16. Alexander, S. **1989.** *Physical Review B*, **40**(11): 7953-7965.
17. Song, X., Jiang, N., Li, Y., Xu, D. and Qiu, G. **2008.** *Chem. Phys*. **110**: 128–135.
18. Twej, W. A. A. **2013**. *JNCS*, **382**: 45–51.
19. Wesam A. A. Twej • Ashraf M. Alattar • Matthew Drexler • Faisal M. Alamgir. **2017**. Tuned optical transmittance in single-step-derived silica aerogels through pH-controlled microstructure. Int Nano Lett (2017) **7**: 257–265.